Problem A: Circumbinary Planets

Team 759

16 November 2014

Abstract

In this paper, we analyze the 3-body problem in order to find possible stable orbits for a small planet orbiting around two stars of masses m_1 and m_2. We first derive the equations of motion for the two-star system in the absence of external forces. Following this solution, we find the potential in a rotating reference frame and identify the five Lagrange points, and observe that they do not offer long-term stability. Because the three body problem lacks an analytical solution, we proceed to simulate the orbits of the binary star system, and then add in a planet with varying initial conditions. We observe stable orbits in the point-mass limit and chaotic, yet potentially stable orbits in the case of smaller radii from the center of mass. Additionally we lend credence to our analytic argument for instability of the Lagrange points by observing the orbit of the planet starting at L_1. Finally, we discuss the limitations of our model.

1 Interpreting the Problem

For this problem, we consider the motion of three celestial objects: Two stars, with masses 1.0 and 0.5 times the mass of the sun ($1.99 \times 10^{30} kg$), and a circumbinary planet with comparatively negligible mass. We are given the period of the binary star system as 30 Earth-days. As an instance of the three-body problem, the closed form solution for this problem is unattainable. Our task is to identify numerically feasible orbits by constraining the system and conducting simulations to model the system's behavior over time.

For our purposes, we constrain the orbits to a single plane, an assumption that is well founded in the results of modern astrophysical literature. Moreover, we assume that both stars and our planet are spherically symmetric, and that the radii of the stars are small compared to the orbital radius. In addition, we take the planet to be orders of magnitude smaller than that of the stars - namely, the mass of the Earth (5.97×10^{24}).

2 Background

2.1 Summary of Concepts

The combined system of a circumbinary planet and its two stars is an example of three-body motion. More generally, this represents a special case of the N-Body problem, which seeks solutions in the form of stable orbits for systems involving N objects under the influence of gravity. It is well understood that the N-body problem has 6N variables (3 position and 3 velocity), where N represents the number of bodies in the system. Although these can be reduced by choice of coordinate and symmetries, even the three-body problem remains unsolved. This problem, in its many variants, has captivated the world of Physics through its terse, and often analytically intangible systems of equations. Nonetheless, computer simulations have provided a framework for deriving various theoretical solutions. Furthermore astrophysicists have used adaptive optics and Doppler Effect analysis as tools to better understand orbital dynamics in multi stellar systems.

2.2 Understanding the Two-Body Problem

Before we foray into circumbinary orbits, we must first delve into the Two-Body Problem. This will give us a first approximation for the motion of the two stars, in the event that the planet is much less massive than either of the stars, so its gravitational pull is negligible. Later, we will consider the effect of the planet's mass on the system's motion, but for now this is a reasonable assumption to make, as most planets in multistellar systems are orders of magnitude less massive than the stars around which they orbit.

2.2.1 Equations of Motion

Here, we will derive out the essential equations of motion for a two-body system under the effects of gravity. We shall designate the stars A and B, and their masses m_A and m_B. Without loss of generality, we can choose an origin O, and define the positions relative to that origin as $\vec{r}_A$ and $\vec{r}_B$ respectively.

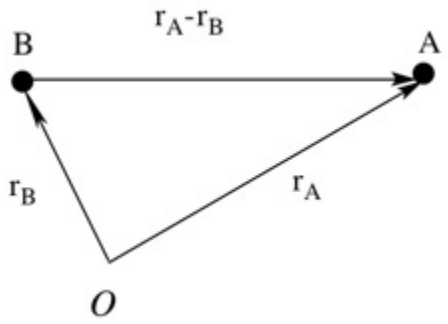

Figure 1: Relative positions of A and B. From the diagram, it is easy to see that taking $\vec{r}$ to be $\vec{r}_A - \vec{r}_B$ gives the difference in positions of the two stars.

The potential energy due to gravity is

$$U(\vec{r}_A, \vec{r}_B) = \frac{-Gm_Am_B}{|\vec{r}_A - \vec{r}_B|} \tag{1}$$

Substituting in $\vec{r} = \vec{r}_A - \vec{r}_B$ gives the simplified relation

$$U(\vec{r}) = \frac{-Gm_Am_B}{|\vec{r}|} \tag{2}$$

Switching to the center of mass frame will also simplify our analysis, because this reference frame provides a translational symmetry. By Noether's theorem, momentum is conserved. it is trivial to see that the center of mass is

$$\vec{R} = \frac{m_A\vec{r}_A + m_B\vec{r}_B}{m_A + m_B} \tag{3}$$

Thus, the kinetic energy T can be written as

$$T = \frac{1}{2}\Big(m_A\dot{\vec{r}}_A^{\,2} + m_B\dot{\vec{r}}_B^{\,2}\Big) = \frac{1}{2}\Big((m_A + m_B)\dot{\vec{R}}^2 + (\frac{m_Am_B\dot{\vec{r}}^{\,2}}{m_A + m_B})\Big) \tag{4}$$

If we let $\mu = \frac{m_Am_B}{m_A+m_B}$, then this becomes

$$T = \frac{1}{2}\Big((m_A + m_B)\dot{\vec{R}}^2 + (\mu\dot{\vec{r}}^{\,2})\Big) \tag{5}$$

Now that we have the potential (2) and the kinetic energy (5) with respect to $\vec{r}$ and $\vec{R}$, we can proceed to set up the Lagrangian $\mathcal{L}$, which we can use to solve the equations of motion.

$$\mathcal{L} = T - U = \frac{1}{2}\Big((m_A + m_B)\dot{\vec{R}}^2 + (\mu\dot{\vec{r}}^{\,2})\Big) + \frac{Gm_Am_B}{|\vec{r}|} \tag{6}$$

By conservation of momentum, $\dot{\vec{R}}$ is constant, so the coordinate is 'ignorable', and we can turn our attention to $\dot{\vec{r}}$. We assume in this analysis that the stars both move in a plane, so that our problem is pared down to two coordinates, and we can represent $\vec{r}$ in polar coordinates as a function of r and ϕ.

$$\vec{r} = \vec{r}(r, \phi) \tag{7}$$

Hence, the Lagrangian can be written as

$$\mathcal{L} = T - U = \frac{1}{2}\Big((m_A + m_B)\dot{\vec{R}}^2 + \mu(\dot{r}^2 + r^2\dot{\phi}^2)\Big) + \frac{Gm_Am_B}{|r|} \tag{8}$$

We can then solve the Euler Lagrange equations

$$\frac{d}{dt}\frac{\partial\mathcal{L}}{\partial\dot{\phi}} = \frac{\partial\mathcal{L}}{\partial\phi} \tag{9}$$

$$\frac{d}{dt}\frac{\partial\mathcal{L}}{\partial\dot{r}} = \frac{\partial\mathcal{L}}{\partial r} \tag{10}$$

Solving the Angular Equation (9), we get

$$\frac{\partial\mathcal{L}}{\partial\phi} = \mu r^2\dot{\phi} = \ell_z \tag{11}$$

where ℓ_z, the z component of the angular momentum, is constant[1]. Solving the Radial Equation (10), and substituting in (11) for $\dot{\phi}$, we get

$$\mu\ddot{r} = \frac{\ell_z^2}{\mu r^3} - \frac{Gm_Am_B}{r^2} \tag{12}$$

Now, we will use these equations to describe r in terms of ϕ. To do this, we must perform the substitution

$$u = \frac{1}{r} \tag{13}$$

and notice that

$$\frac{d}{dt} = \frac{d\phi}{dt}\frac{d}{d\phi} = \frac{\ell_z u^2}{\mu}\frac{d}{d\phi} \tag{14}$$

which allows us to write

$$u"(\phi) = -u(\phi) + \frac{\mu Gm_Am_B}{\ell_z^2} \tag{15}$$

Because the force of gravity obeys the inverse square law, all coordinate dependence drops out of the final term, leaving it as a constant, and enabling us to solve this differential equation analytically[1]. Letting

$$w(\phi) = u(\phi) - \frac{\mu G m_A m_B}{\ell_z^2} \tag{16}$$

we find that

$$w"(\phi) = -w(\phi) \tag{17}$$

which is the differential equation for a simple harmonic oscillation with solution

$$w(\phi) = Acos(\phi - \delta) \tag{18}$$

for some constant A. By choosing a convenient orientation, we can set δ to 0. We can then perform the necessary substitutions to express the equation in terms of u, and finally in terms of r.

$$\vec{r}(\phi) = \frac{c}{1 + \epsilon \cos\phi}\hat{r} \tag{19}$$

where $c = \frac{\ell_z^2}{\mu G m_A m_B}$, and ϵ is the eccentricity of the orbit defined by

$$0 < \epsilon = \frac{A\ell_z^2}{\mu G m_A m_B} < 1 \tag{20}$$

for bounded orbits. Furthermore, we can use (19) and (3), combined with the fact that $\vec{R} = 0$ in the center of mass frame to get the equations for $\vec{r}_A$ and $\vec{r}_B$.

$$\vec{r}_A(\phi) = \frac{m_B}{m_A + m_B}\frac{c}{1 + \epsilon \cos\phi}\hat{r} \tag{21}$$

$$\vec{r}_B(\phi) = -\frac{m_A}{m_A + m_B}\frac{c}{1 + \epsilon \cos\phi}\hat{r} \tag{22}$$

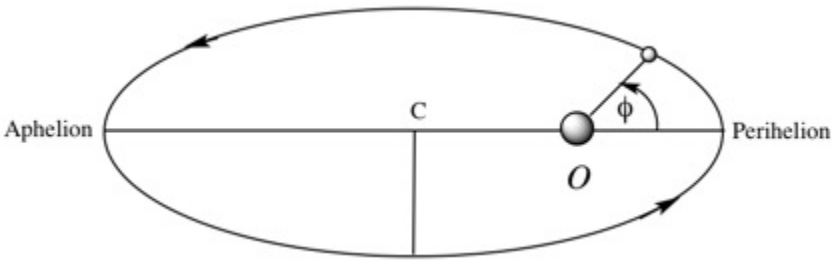

Figure 2: Example of a bounded elliptical orbit satisfying the equations of section 2.2. r_{min} is the distance between the origin, O, and the perihelion, and r_{max} is distance between the origin and the aphelion.

3 Formulating the Three-Body Problem

Now that we understand the dynamics resulting from the two-body Problem, we can extrapolate to N-particles - in our case 3 - by generalizing our approach. First, we look at the three-body problem. Then we look at the restricted three-body problem, in which one of the three objects has negligible mass. Finally, we proceed to analyze the stability of the 5 resulting Lagrange points.

3.1 The Three-Body Problem

In a system with N point-masses, we can index objects with i, such that object i has mass m_i, radius $\vec{r}_i$ from the designated origin, and velocity $\dot{\vec{r}}_i$, with $1 \leq i \leq N \in \mathbb{Z}$. In order to find the motion of the point-masses, we must solve a system of N coupled force equations, the i^{th} of which is given by[2]

$$m_i \frac{d^2\vec{r}_i}{dt^2} = \sum_{j \neq i}^{N} G m_i m_j \frac{\vec{r}_j - \vec{r}_i}{||\vec{r}_j - \vec{r}_i||^3} \tag{23}$$

For $N = 3$ we have a system of 9 coupled differential equations:

$$\frac{d^2\vec{r}_1}{dt^2} = Gm_2 \frac{\vec{r}_2 - \vec{r}_1}{||\vec{r}_2 - \vec{r}_1||^3} + Gm_3 \frac{\vec{r}_3 - \vec{r}_1}{||\vec{r}_3 - \vec{r}_1||^3} \tag{24}$$

$$\frac{d^2\vec{r}_2}{dt^2} = Gm_1 \frac{\vec{r}_1 - \vec{r}_2}{||\vec{r}_1 - \vec{r}_2||^3} + Gm_3 \frac{\vec{r}_3 - \vec{r}_2}{||\vec{r}_3 - \vec{r}_2||^3} \tag{25}$$

$$\frac{d^2\vec{r}_3}{dt^2} = Gm_1 \frac{\vec{r}_1 - \vec{r}_3}{||\vec{r}_1 - \vec{r}_3||^3} + Gm_2 \frac{\vec{r}_2 - \vec{r}_3}{||\vec{r}_2 - \vec{r}_3||^3} \tag{26}$$

3.2 Restricted Three-Body Problem

The three-body problem can be simplified if one of the objects is significantly less massive than the other masses. Without loss of generality, assume this text itlight body to be the third object. This decouples equations (24) and (25), giving the expressions[3]

$$\frac{d^2\vec{r}_1}{dt^2} = Gm_2 \frac{\vec{r}_2 - \vec{r}_1}{||\vec{r}_2 - \vec{r}_1||^3} \tag{27}$$

and

$$\frac{d^2\vec{r}_2}{dt^2} = Gm_1 \frac{\vec{r}_1 - \vec{r}_2}{||\vec{r}_1 - \vec{r}_2||^3} \tag{28}$$

To simplify the analysis even further, assume that the third object moves in the same plane as the two massive objects. We know from Part 2 that the angular momentum of the first two objects around the center of mass is constant. Thus, it makes sense to transform from

a *sidereal* frame into a *synodic* frame. Choosing t such that $t = 0$ when the *sidereal* and *synodic* axes coincide, we can relate the two coordinate systems for the third object:

$$x(t) = x'(t)cos(t) - y'(t)sin(t) \tag{29}$$

$$y(t) = x'(t)sin(t) - y'(t)cos(t) \tag{30}$$

Taking two time derivatives gives the equations relating the second derivatives:

$$\ddot{x} = \ddot{x}'cos(t) - 2\dot{x}'sin(t) - x'cos(t) - \ddot{y}'sin(t) - -2\dot{y}'cos(t) + y'sin(t) \tag{31}$$

$$\ddot{y} = \ddot{x}'sin(t) + 2\dot{x}'cos(t) - x'sin(t) + \ddot{y}'cos(t) - 2\dot{y}'sin(t) - y'sin(t) \tag{32}$$

Solving these equations, we get the synodic accelerations:

$$\ddot{x}cos(t) + \ddot{y}sin(t) = \ddot{x}' - x' - 2\dot{y}' \tag{33}$$

$$-\ddot{x}sin(t) + \ddot{y}cos(t) = \ddot{y}' - y' + 2\dot{x}' \tag{34}$$

If we substitute in the gravitational values of the sidereal accelerations, and let $\alpha = \frac{m_2}{m_1+m_2}$, and $G(m_1 + m_2) = 1$, then we can express the effective potential in the synodic frame as[3]

$$U(x', y') = -\frac{1-\alpha}{\sqrt{(x'-\alpha)^2 + y'^2}} - \frac{\alpha}{\sqrt{(x'+1-\alpha)^2 + y'^2}} - \frac{x'^2 + y'^2}{2} \tag{35}$$

3.3 Analysis of Lagrange Point Stability

Our analysis of the restricted three-body problem gave us the effective potential of the system in the synodic frame. In order to find equilibrium positions, we must find the values at which the potential is extremized. In other words, we want the values that satisfy the equation

$$\nabla U = 0 \tag{36}$$

These 'equilibrium' positions, of which there are five, are called Lagrange points[4]. As shown in Figure 3 below, the first three Lagrange points, L_1, L_2, and L_3 all lie on the straight line joining the two large masses[5].

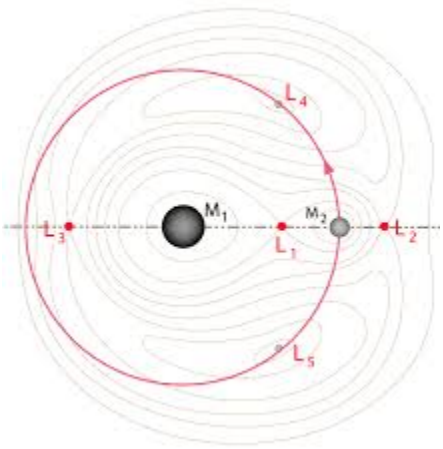

Figure 3: Lagrange points as equilibrium solutions to the restricted three-body problem. The overlaid potential shows the points where $\nabla U = 0$. (Courtesy HyperPhysics).

L_1 occurs at the location where the centrifugal and gravitational forces balance each other. At this point, the equation

$$\frac{m_1}{(R-r_1)^2} = \frac{m_2}{r_1^2} + \left(\frac{m_1}{m_1+m_2}R - r_1\right)\frac{m_1+m_2}{R^3} \tag{37}$$

is satisfied, where R represents the distance between the two massive objects. At first approximation, the solution is

$$r_1 \approx R\sqrt[3]{\frac{m_2}{3m_1}} \tag{38}$$

L_2 occurs at the location where gravity balances inertia. At this point, the equation

$$\frac{m_1}{(R+r_2)^2} + \frac{m_2}{r_2^2} = \left(\frac{m_1}{m_1+m_2}R + r_2\right)\frac{m_1+m_2}{R^3} \tag{39}$$

As is shown in Figure 3, $r_1 \approx r_2$. This is reflected in the fact that, to first approximation,

$$r_2 \approx R\sqrt[3]{\frac{m_2}{3m_1}} \tag{40}$$

L_3 represents the solution to another equation balancing centrifugal and gravitational forces:

$$\frac{m_1}{(R-r_3)^2} + \frac{m_2}{(2R-r_3)^2} = \left(\frac{m_2}{m_1+m_2}R + R - r_3\right)\frac{m_1+m_2}{R^3} \tag{41}$$

To a first order approximation,

$$r_3 \approx R\frac{7m_2}{12m_1} \tag{42}$$

Although all three of these Lagrange points are equilibrium positions, they are unstable, as $\frac{d^2U}{dr^2} < 0$. L_4 and L_5, however, the points that are equidistant from both masses, are given

by[6] $$L_4 = \left(\frac{R}{2}\left(\frac{m_1 - m_2}{m_1 + m_2}\right), \frac{\sqrt[3]{3}}{2}R\right) \quad (43) \qquad L_5 = \left(\frac{R}{2}\left(\frac{m_1 - m_2}{m_1 + m_2}\right), -\frac{\sqrt[3]{3}}{2}R\right) \quad (44)$$

They are stable if the following conditions[6] are met:

$$\left(\frac{m_1 - m_2}{m_1 + m_2}\right)^2 \geq \frac{23}{27} \qquad \sqrt{27\left(\frac{m_1 - m_2}{m_1 + m_2}\right)^2 - 23} \leq 2$$

3.3.1 Calculating the Lagrange Points of Our System

Now that we have the positions of equilibria for the restricted three-body problem, we can plug in the specific conditions of our binary star system: $m_1 = m_{sun} = 1.99 \times 10^{30} kg$, and $m_2 = \frac{m_{sun}}{2} = 0.995 \times 10^{30} kg$. For the sake of simplicity, take $R = 1$.

Table 1: Positions of Lagrange Points

Lagrange Point	Position in units of R
L_1	$(\sqrt[3]{\frac{1}{6}}, 0)$
L_2	$(\sqrt[3]{\frac{1}{6}}, 0)$
L_3	$(\frac{7}{24}, 0)$
L_4	$(\frac{1}{6}, \frac{\sqrt[3]{3}}{2})$
L_5	$(\frac{1}{6}, -\frac{\sqrt[3]{3}}{2})$

Plugging the masses m_1 and m_2 into the stability condition, it is easy to see that L_4 and L_5 are not stable. Thus, although each Lagrange point is an equilibrium of our binary star system, none are stable.

4 The Binary-Star Point-Mass Limit

Having established in the previous section that the Lagrange points presented only unstable equilibrium, we sought another simple model by which to generate possible points of stability.

For a planet orbiting around the two stars at a great enough radius, the distance between the two stars would become insignificant, and the stars could together be treated

as one point-mass. At this large radius of $r >> r_{max}$, where r_{max} is the maximum distance between the two stars in their elliptical orbits, assuming the eccentricity $\epsilon \neq 1$, then the planet would approximately revolve around the center of mass of the two stars in an ellipse, as detailed in Section 2. In particular, if the eccentricity is close to 0, then the resulting orbit is quasi-circular and its motion satisfies the approximate equality of gravitational and centripetal forces:

$$\frac{m\dot{r}^2}{r} \approx \frac{Gm(m_1 + m_2)}{r^2} \tag{45}$$

resulting in velocity

$$\dot{r} \approx \sqrt{\frac{G(m_1 + m_2)}{r}} \tag{46}$$

5 Simulations Using Python

5.1 Motivation

In order to better understand the mechanics of the proposed problem, and in light of the dearth of analytic solutions we ran a number of 3-body simulations involving various initial conditions. We hoped through these simulations to validate our results regarding the instability of the Lagrange points, and the stability of quasi-circular orbits.

5.2 Assumptions, Initial Conditions, and Implementation

We started by creating a simulation for the motion of the 2 stars using the analytic solution presented in (21) and (22). Plotting these solutions gives:

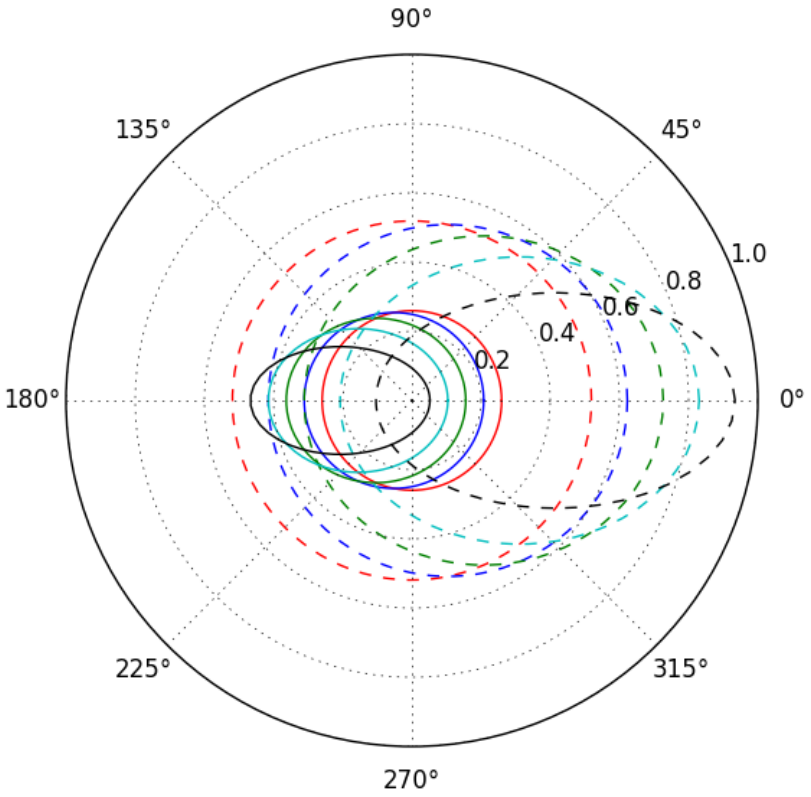

Figure 4: Elliptical solutions to the two body problem. The trajectory of the star with less mass, m_2 is shown with the dotted lines while that of the more massive star, with mass m_1, is displayed using solid lines. Eccentricity of 0.0 corresponds to blue, 0.2 to green, 0.4 to red, 0.6 to cyan, and 0.8 to red.

The positions of both stars can be described in terms the orbital angle ϕ. This dependence, however, is not ideal. Instead, we prefer to relate the position vector to time. This is given by the following relationship between time elapsed since perihelion and ϕ:[7]

$$t(\phi) = \frac{\tau}{2\pi}\left[2\arctan\left(\sqrt{\frac{1-\varepsilon}{1+\varepsilon}}\right)\tan\left(\frac{\phi}{2}\right) - \frac{\varepsilon\sqrt{1-\varepsilon^2}\sin(\phi)}{1+\varepsilon\cos(\phi)}\right] \tag{47}$$

Because we will be determining the position of the planet via numerical integration of the acceleration, we need to determine ϕ's dependence on time. Rearranging the above transcendental equation to creation a function in time has proven to be an exercise in futility. Instead, our first step will be to generate a conversion table for our two variables. To ensure that this table will be able to supply sufficiently accurate numbers, we calculated

10,000 time-angle pairs over a single cycle. Inverting the dependence and plotting angle as a function of time:

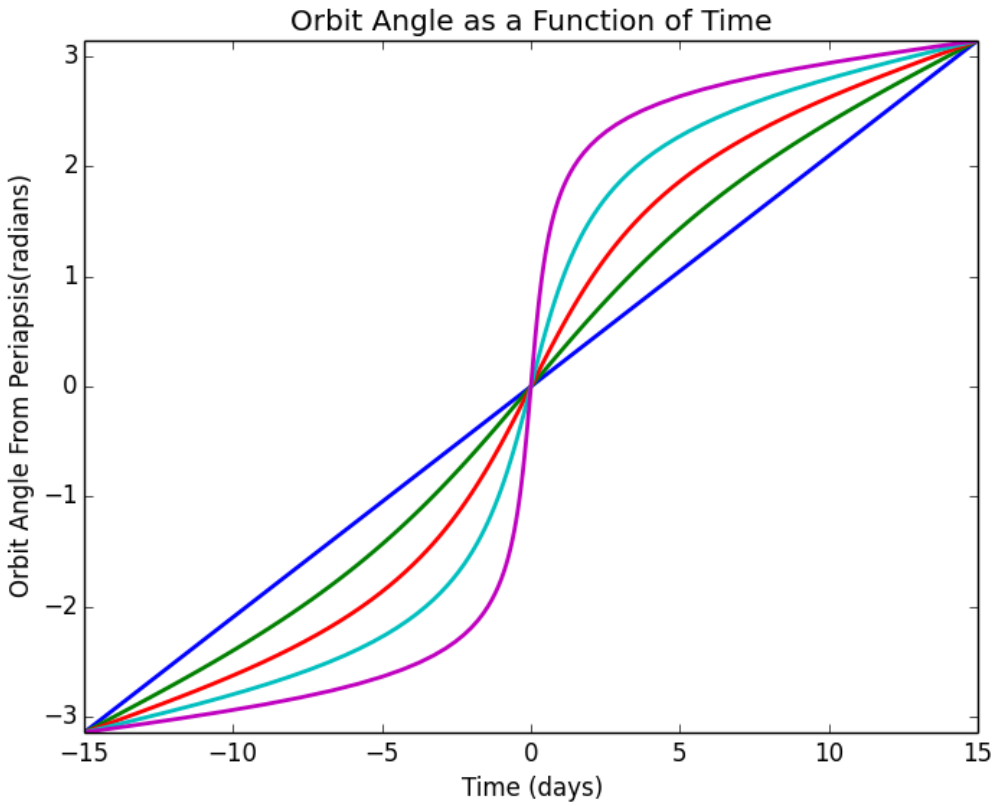

Figure 5: Orbital angle as a function of time for varying eccentricities. Eccentricity of 0 corresponds to blue, 0.2 to green, 0.4 to red, 0.6 to cyan, and 0.8 to red.

As expected, the orbital velocity (slope) at the perihelion ($\phi = 0$, $t = 0$) is maximized with larger eccentricities. With a time dependence table we graphically demonstrate the evolution of the elliptical orbits of the stars as functions of time.

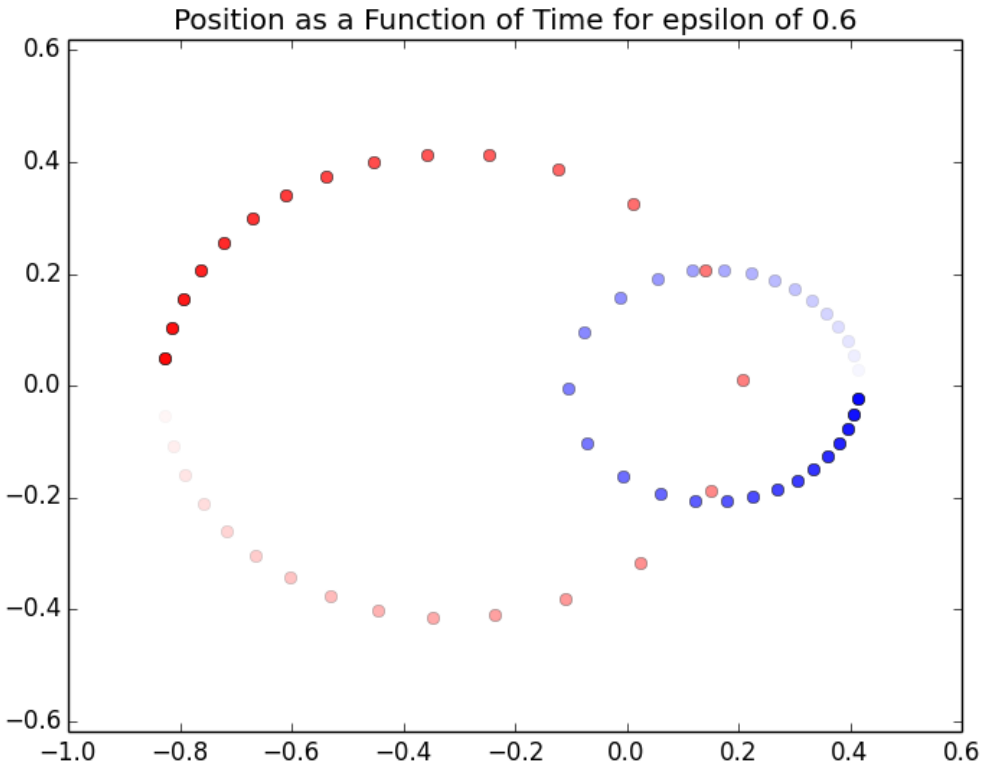

Figure 6: Evolution of binary star system as a function of time with an eccentricity of 0.6

With the stellar dynamics fully simulated, we move then to the next step of introducing a planet into the system. In this simulation, we assume the planet is of negligible mass with respect to the masses of both stars. As a result, we do not account for perturbations in the elliptical orbits of the stars due to gravitational effects of the planet. By noting the relationship between the constant angular momentum and the eccentricity, (21) and (22), it is possible to describe a spectrum of angular momenta with different values for ϵ.

The code, which is presented in appendix A, is a class based program written in python with the added benefit that it allows for the easy addition of bodies to the simulation.

5.3 Results

First, we simulated the motion of the system with the planet situated at the first Lagrange point, L_1. The planet rapidly devolved into ejection from orbit (Figure 8 in Appendix B). This corroborated the analytic expectation that although L_1 and L_4 are equilibrium

positions, they are unstable.

We proceeded to test our hypothesis regarding the point-mass limit under different eccentricities. We tested a variety of eccentricities for $r = 150 \times 10^9 meters$, and $r = 450 \times 10^9 meters$, three times as far away from the center of mass of the system. Examining a range of values for ϵ, we determined that, for eccentricities of 0.0 up to at least 0.9, velocities close to (46) produced stable orbits. Furthermore, we noticed, (Figures 9a-f in Appendix B) that greater radii produced more predictable, elliptical motion. In particular, when the radius was large, and velocities close to (46), the orbits tended to circles. The adhered to our expectation for the behavior of the system in the point-mass limit.

6 Limitations of our Model

In our analysis of the stability of orbits for the circumbinary planet, we made many assumptions and simplifications that limit the general nature of our solutions. We assume from the beginning that all three celestial bodies are spherically symmetric, allowing us to treat them as point-masses. We also assume that the mass of the planet is significantly smaller than the masses of the stars, which enables us to make use of the restricted three-body problem. If this mass is not negligible, then our discussion of Lagrange points is entirely unfounded. In addition, even small planetary masses will cause perturbations in the elliptical orbits of the binary stars, complicating the dynamics of the system.

If the radius in the point-mass approximation is not sufficiently large, then the orbit deviates from a perfect ellipse around the center of mass of the system. This comes as no surprise, as the motions of Figure 8 are fairly tame compared to those of the more chaotic system portrayed in Figure 9. We also implicitly assume that the radii of the stars do not pass the first Lagrange point, so there is no mass spillover.

Another limitation of our model takes the motion of the planet as being entirely in the plane containing the stars, thereby narrowing our view of the problem.

Conclusion

Although our solutions are in no way complete, we predict a number of stable orbits for circumbinary planets given our simulations in Python. We describe the elliptical orbits of two-body motion and derive the five Lagrange points in the two body system which represent equilibrium locations. However, further analysis reveals under the mass constraints given in the problem, none of the orbits resulting from these Lagrange points are stable. We next look at the case in which our planet is far away from the stars. In this limit, the binary star system looks like a single point-mass and we can again apply the solutions of the two-body problem. To further confirm that our predictions were valid, we simulated

the 3-body problem in Python. In general, we show a large set of solutions resulting from a variety of initial conditions and parameters.

Appendix A

```
import numpy as np
import matplotlib.pyplot as plt

resolution = 10000 #over sample to determine close relationship between phi and time
period = 30 #period of stars in days
eps = 0 # Eccentricity
xa = np.linspace(-np.pi,np.pi,resolution) #array of angles from -pi to pi
xb = xa + np.pi #offset y b/c it will be plotting the negitive radii
s = np.sin(xa) #Sine value for each angle
c = np.cos(xa) #Cosine value for each angle
ta = np.tan(xa/2) #Tangent value for each angle

##tphi is part of a look-up table which relates times to the angles in x
tphi = period/(2*np.pi) * (2*np.arctan(np.sqrt((1-eps)/(1+eps))*ta) - eps*np.sqrt(1-eps**2)*s/(1+eps*c))

###CLASS PLANET HANDLES CALCULATION OF THE PLANET'S MOTION
class planet(object):
        ## endow
        def __init__(self):
                self.xvelocity = 0#m/s
                self.yvelocity = 0#m/s
                self.xpos = .225*10**11#m
                self.ypos = .974*10**11#150*10**9#m

        def calc_accel(self, starAXpos, starAYpos, starBXpos, starBYpos):
                ## distance in one component direction from the star
                diffAx = self.xpos-starAXpos
                diffAy = self.ypos-starAYpos
                diffBx = self.xpos-starBXpos
                diffBy = self.ypos-starBYpos
                self.distAsq = (diffAx)**2 + (diffAy)**2
                self.distBsq = (diffBx)**2 + (diffBy)**2
                self.accelmagA = -6.674*10**(-11)*.5*1.99*10**(30)/self.distAsq
                self.accelmagB = -6.674*10**(-11)*1.99*10**(30)/self.distBsq
                self.xaccel = diffAx*self.accelmagA/np.sqrt(self.distAsq) + diffBx*self.accelmagB/np.sqrt(self.distBsq)
                self.yaccel = diffAy*self.accelmagA/np.sqrt(self.distAsq) + diffBy*self.accelmagB/np.sqrt(self.distBsq)

        def calc_velo(self):
                self.xvelocity = self.xvelocity + self.xaccel*tstep*30*24*3600
                self.yvelocity = self.yvelocity + self.yaccel*tstep*30*24*3600

        def calc_change_pos(self):
                self.xdelta = self.xvelocity*tstep*30*24*3600
                self.ydelta = self.yvelocity*tstep*30*24*3600

        def calc_pos(self):
                self.xpos = self.xpos + self.xdelta
                self.ypos = self.ypos + self.ydelta


def find_index_nearest(array,value):
    idx = (np.abs(array-value)).argmin()
    return idx
```

```
##Initiailize Planet Object
Planet = planet()
videores = 5000 #how many samples per simulation
numstar_periods = 10 #how many solar periods
tvals = np.linspace(0,numstar_periods*period,videores) #list of times for which thepositions will be evaluated
tstep = (numstar_periods*period)/float(videores) #how much time between each time step
picfreq = 4 #how many samples per "snapshot"
pot = [] #init list for second dervitives

fig = plt.figure(figsize=(6,6))

for i in range(videores):
        s = tvals[i] #get time from list of choosen times
        t = (s)%period-period/2 # b/c catalog goes from -period/2 to period/2, convert to between this range

        ##find angle for given time in catalogue
        anglea = xa[find_index_nearest(tphi, t)]
        angleb = xb[find_index_nearest(tphi, t)]

        ##Calculate radius from Angle
        ra = -(.77845*(eps**2-1))/(1-eps*np.cos(angleb))*2/3*150*10**9#m .5 solar masses
        rb = -(.77845*(eps**2-1))/(1-eps*np.cos(angleb))*1/3*150*10**9#m 1 solar mass

        ##Convert to Rectangular Coordinates
        xapos = np.cos(anglea)*ra
        yapos = np.sin(anglea)*ra
        xbpos = np.cos(angleb)*rb
        ybpos = np.sin(angleb)*rb

        ##Calculate Position, Velocity, and Acceleration to determine orbit and stability
        Planet.calc_change_pos()
        Planet.calc_pos()
        Planet.calc_accel(xapos,yapos,xbpos,ybpos)
        Planet.calc_velo()

        if (i%picfreq == 0):
                ##Plot Star and Planet Positions
                ax = fig.add_subplot(1,1,1) #Subplot for picture
                ax.plot([xapos],[yapos],"r.")#, alpha = float(i)/videores)#, color = str(color[t]))
                ax.plot([xbpos],[ybpos],"b.")#, alpha = float(i)/videores)#, color = color[t])
                ax.plot([Planet.xpos],[Planet.ypos],"g.")

                ##Set axes
                scale = 2*10**11
                plt.axis([-scale,scale,-scale,scale])
                name = "Position as a Function of Time for epsilon of %3.2f" %(eps)
                plt.title(name)
                plt.xlabel('X-Coordinate (Astronomical Units)')
                plt.ylabel('Y-Coordinate (Astronomical Units)')

                name = '3body6/' + '0'*(4-len(str(i/picfreq))) + str(i/picfreq) + '.png'
                plt.savefig(name)
```

Appendix B

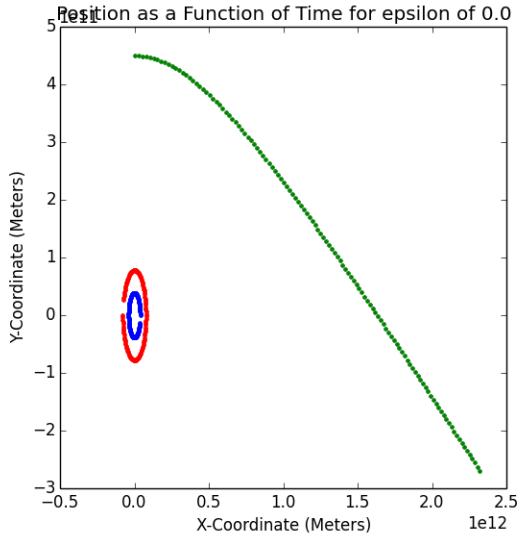

Figure 7: A planet initially placed at $r = 450 \times 10^9$ meters from the center of mass with a large velocity exits the system.

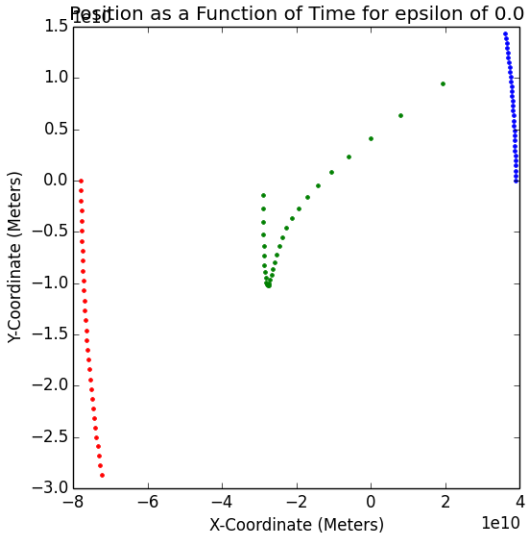

Figure 7: Time evolution of a planet in a binary star system starting at L_1 with 0 initial velocity. As the equations of the restricted three-body problem would suggest, this position is unstable, and the planet is ejected.

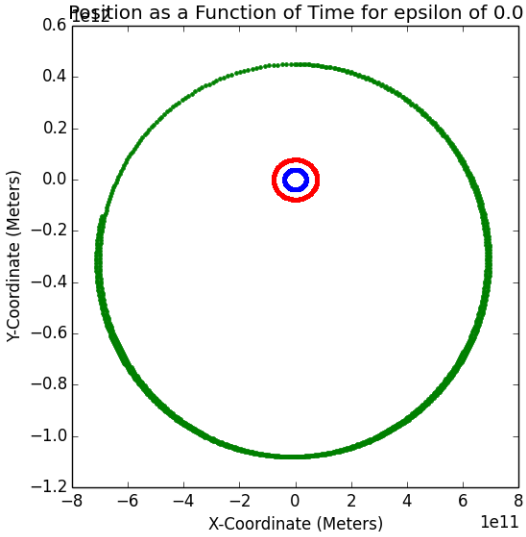

Figure 8a: Time evolution of a planet in the point-mass limit with $r = 450 \times 10^9$ meters and $\epsilon = 0.0$. The path traced out by the planet is nearly periodic.

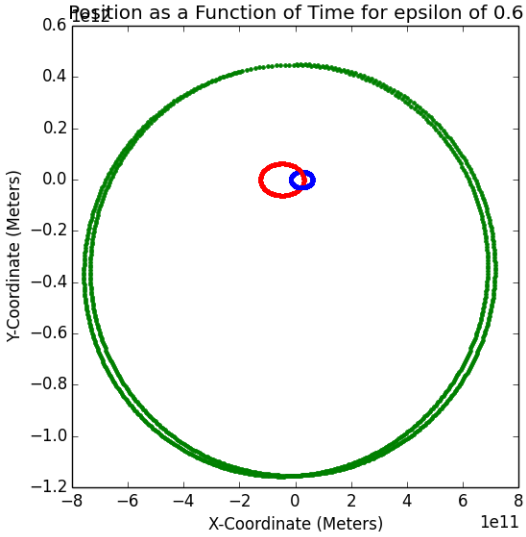

Figure 8b: Time evolution of a planet in the point-mass limit with $r = 450 \times 10^9$ meters and $\epsilon = 0.6$.

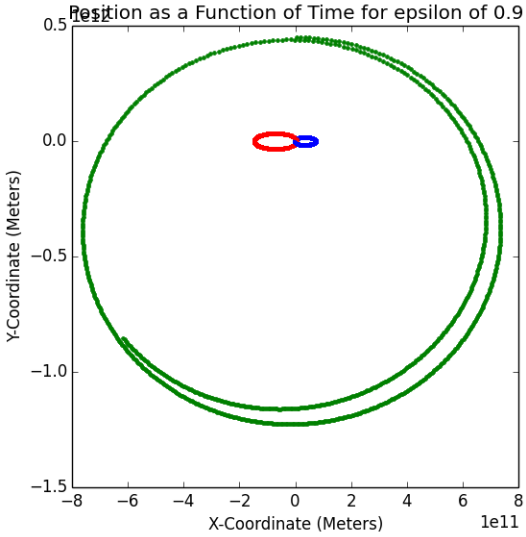

Figure 8c: Time evolution of a planet in the point-mass limit with $r = 450 \times 10^9$ meters and $\epsilon = 0.9$.

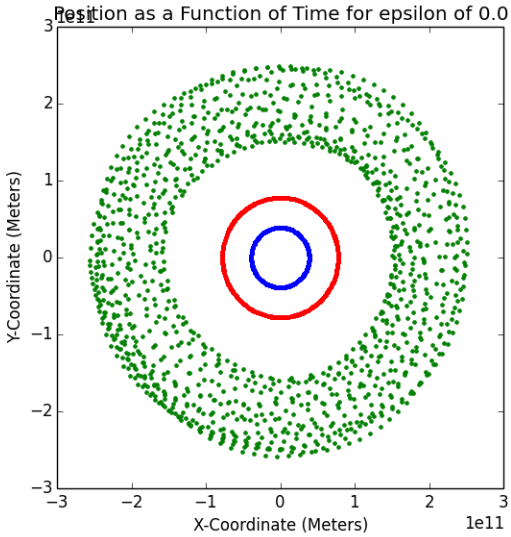

Figure 9a: Time evolution of a planet in the point-mass limit with $r = 150 \times 10^9$ meters and $\epsilon = 0.0$. The path traced out by the planet is nearly periodic.

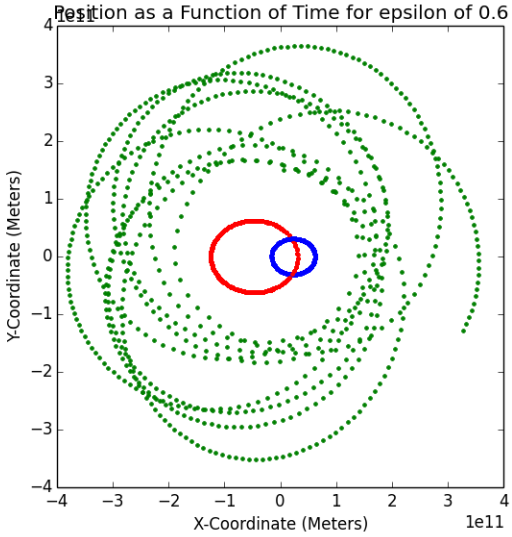

Figure 9b: Time evolution of a planet in the point-mass limit with $r = 150 \times 10^9$ meters and $\epsilon = 0.6$.

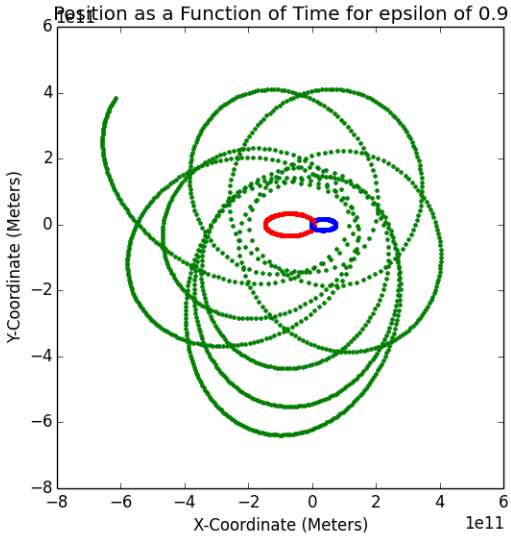

Figure 9c: Time evolution of a planet in the point-mass limit with $r = 150 \times 10^9$ meters and $\epsilon = 0.9$.

Appendix C

Kepler's Third law gives us:

$$\tau^2 = \frac{4\pi^2 \mu a^3}{GM_1M_2} \tag{48}$$

Where τ is the orbital period of the two bodies, μ is the reduced mass defined above, and a is the semi-major axis given by:

$$a = \frac{c}{1-\epsilon^2} \tag{49}$$

where ϵ is the eccentricity, and c is $c = \frac{\ell_z^2}{\mu G m_A m_B}$. Putting these three equations together, we get an equation in just ϵ and ℓ

$$\tau^2 = \frac{4\pi^2\mu}{GM_1M_2}\frac{1}{(1-\epsilon^2)^3}\left(\frac{\ell^2}{\mu GM_1M_2}\right)^3 \tag{50}$$

$$\ell = \sqrt[3]{\frac{(1-\epsilon^2)^3\tau^2G^4M_1^4M_2^4\mu^3}{4\pi^2\mu}} \tag{51}$$

$$\ell = (1-\epsilon^2)GM_1M_2\mu\sqrt[3]{\frac{\tau^2GM_1M_2}{4\pi^2\mu}} \tag{52}$$

Thus, given any bounded orbit ($1 > \epsilon > 0$), ℓ will give the necessary angular momentum.

References

[1] John R. Taylor *Classical Mechanics*. 2005, "University Science Books".

[2] A. Chenciner. "Three Body Problem" *Scholarpedia* 2.10 (2007): 2111.

[3] Richard J. Gonsalves. *The Gravitational Three Body Problem*. 2011, http://www.physics.buffalo.edu/phy410-505/2011/topic2/app2/.

[4] Bradley W. Carroll, and Dale A. Ostlie. *An Introduction to Modern Astrophysics*. 2007, "Pierson Education, Inc.".

[5] Richard Fitzpatrick. *Lagrange Points*. 2011, http://farside.ph.utexas.edu/teaching/336k/Newtonhtml/node

[6] Neil J. Cornish *The Lagrange Points*. http://www.physics.montana.edu/faculty/cornish/lagrange.pdf.

[7] Shane L. Larson. *The Kepler Equation*. March 2012,

[8] Robert A. Braeunig. *Orbital Mechanics*. 2013, http://www.braeunig.us/space/orbmech.htm.

[9] Brenton Duffy. *Analytical and Numerical Methods for the Elliptic Restricted Three-Body Problem of Astrodynamics* April 2012,